Wideband Synthetic Aperture Beamforming for Through-the-Wall Imaging

Moeness G. Amin and Fauzia Ahmad

Through-the-wall radar imaging (TWRI) and sensing is emerging as an important area of research and development [1]-[6]. A TWRI system provides enhanced situational awareness in operational environments for a variety of civilian and military applications. In particular, a TWRI system facilitates real-time information-gathering and intelligent decision-making about the contents of the indoor scene. Compared to other radar applications, TWRI faces unique challenges due to signal propagation through walls. The composition and thickness of the wall, its dielectric constant, and the angle of incidence affect the strength and characteristics of the propagating signal. The change in propagation speed and wave refraction must be taken into account for effective and accurate imaging. Failure to do so would cause undesirable errors in determining the nature and the locations of the targets behind walls. In this lecture note, we present a synthetic aperture beamforming approach that uses ray perturbation theory to account for the effects of transmission through a single uniform wall.

RELEVANCE

Through-the-wall beamforming discussed in this lecture note, and imaging and sensing through walls, in general, can be used in search and rescue missions, surveillance and reconnaissance, and building clearing operations. The material we present herein fits well into graduate signal processing courses in electrical engineering, such as courses on radar signal processing and array signal processing.

PREREQUISITES

The prerequisites for understanding and using this lecture note include basic linear algebra and introductory signal processing.

PROBLEM STATEMENT

The objective of through-the-wall sensing technology is to provide the ability to ‘see’ through visually opaque materials such as walls and doors. More specifically, a TWRI system should be able to detect the presence of targets behind walls, provide information concerning each target’s location, motion, size, and radar backscattering cross-section (RCS), and finally identify and

classify these targets. Thus, the problem under consideration in this lecture note is determining how many targets are behind the wall, what are their locations, cross-sections and focusing delays.

SOLUTION

DATA ACQUISITION

Consider an *M*-element line array of transceivers. Two different arrangements can be used for aperture synthesis. Either all the elements of the intended array can be physically present and share a single processing channel via a multiplexer, or a single transceiver can be used to realize the full *M*-element array by moving this transceiver to different locations forming the array aperture. Let the wall, through which the system is looking, be uniform with a thickness d and a dielectric constant ε. The wall lies in the (*x*,*y*)-plane, whereas the line array is located parallel to the *x*-axis in the (*x*,*z*)-plane. The array can be placed against the wall or at some standoff distance z_{off}. The region being imaged is located beyond the wall along the positive *z*-axis. Let the *m*-th transceiver, placed at location $\mathbf{x}_{tm} = (x_{tm}, -z_{off})$, illuminate the scene with a wideband signal, $s(t)$. The reflection by any target located in the region being imaged is measured only at the same transceiver location. For the case of a single point target located at $\mathbf{x}_p = (x_p, z_p)$, the signal $r_m(t)$, measured at the *m*-th transceiver is given by

$$r_m(t) = a(\mathbf{x}_p)s(t - \tau_{mp}), \tag{1}$$

where $a(\mathbf{x}_p)$ is the complex reflectivity of the point target and τ_{mp} is the propagation delay encountered by the signal as it travels from the *m*-th transceiver to the target located at $\mathbf{x}_p$, and back to the same transceiver. As shown in Fig. 1, this delay is given by

$$\tau_{mp} = \frac{2l_{mp,air,1}}{c} + \frac{2l_{mp,wall}}{v} + \frac{2l_{mp,air,2}}{c}, \qquad v = \frac{c}{\sqrt{\varepsilon}} \tag{2}$$

Here, c is the speed of light and v is the speed of propagation through the wall and ε is the dielectric constant of the wall. The variables $l_{mp,air,1}$, $l_{mp,wall}$, and $l_{mp,air,2}$ represent the traveling distances of the signal before, through, and beyond the wall, respectively, from the *m*-th transceiver to the target at $\mathbf{x}_p$. This process is repeated at each transceiver location until all *M* locations have been exhausted.

THROUGH-THE-WALL BEAMFORMING

The data measured at the *M* transceivers is processed as follows to generate an image of the scene. The region of interest in the (*x*, *z*)-plane is divided into a finite number of pixels. As shown in Fig. 2, the complex composite signal corresponding to the *q*-th image pixel located at $\mathbf{x}_q = (x_q, z_q)$, is obtained by time delaying and weighting the *M* measurements, and summing the results. The output for a single target case is given by

$$\begin{aligned} y_q(t) &= \sum_{m=1}^{M} w_m r(t + \tau_{mq}) \\ &= \sum_{m=1}^{M} a(\mathbf{x}_p) w_m s(t - \tau_{mp} + \tau_{mq}) \end{aligned} \tag{3}$$

where w_m and τ_{mq} are, respectively, the weight and the focusing delay applied to the output of the *m*-th transceiver. The focusing delay, given by (2) with the target subscript *p* replaced by the image pixel subscript *q*, synchronizes the signal arrivals from the pixel $\mathbf{x}_q$ across the *M* transceivers, and as such allows coherent imaging of the scene. Unlike the focusing delay, the weight, w_m, is independent of the pixel location $\mathbf{x}_q$, and serves to control the shape and sidelobe structure of the system point spread function. The complex amplitude image value $I(\mathbf{x}_q)$ for the pixel located at $\mathbf{x}_q$ is obtained by passing the signal $y_q(t)$ through a filter matched to the transmitted pulse $s(t)$ and sampling the output of the filter as follows,

$$\begin{aligned} I(\mathbf{x}_q) &= (y_q(t) * h(t))\Big|_{t=0} \\ &= \Big(\sum_{m=1}^{M} a(\mathbf{x}_p) w_m s(t - \tau_{mp} + \tau_{mq}) * h(t)\Big)\Big|_{t=0} \end{aligned} \tag{4}$$

where $h(t) = s^*(-t)$ is the impulse response of the matched filter, the superscript * denotes complex conjugate, and '*' denotes the convolution operator. The process, described by (3) and (4), is performed for all pixels in the region of interest to generate the composite image of the scene.

For a scene consisting of *P* point targets, the complex amplitude pixel value, $I(\mathbf{x}_q)$, can be obtained by superposition of the target reflections,

$$I(\mathbf{x}_q) = \left(\sum_{p=1}^{P} \sum_{m=1}^{M} a(\mathbf{x}_p) w_m s(t - \tau_{mp} + \tau_{mq}) * h(t) \right) \Big|_{t=0} \tag{5}$$

The number and locations of the targets can be discerned from the composite image of the scene. The squared magnitude of the image pixel value, corresponding to each target location, provides an estimate of the cross-section of the target.

COMPUTATION OF THE FOCUSING DELAYS

We now formulate the set of equations for the computation of the traveling distances between the transceivers and the pixel locations, and subsequently, the focusing delays, in the presence of the wall, given the exact knowledge of the wall thickness and its dielectric constant. Consider the traveling from the *m*-th transceiver at $\mathbf{x}_{tm}$ to the *q*-th pixel located at $\mathbf{x}_q$. The signal traveling through the air-wall-air interface (ε is normally greater than 1 for most wall materials and it is equal to 1 air) undergoes refraction, as shown in Fig. 1. The angle ψ_{mq} is given by Snell's law as [7]

$$\psi_{mq} = \sin^{-1}\left(\frac{\sin\theta_{mq}}{\sqrt{\varepsilon}} \right) \tag{6}$$

where θ_{mq} is the angle of incidence. From Fig. 1, [7]

$$l_{mp,air,1} = \frac{z_{off}}{\cos\theta_{mq}}, \quad l_{mp,wall} = \frac{d}{\cos\psi_{mq}}, \quad l_{mp,air,2} = \frac{z_q - d}{\cos\theta_{mq}} \tag{7}$$

The coordinates of point **A** in Fig. 1 are $(x_{tm} + z_{off}\tan\theta_{mq}, 0)$. Applying the cosine law to the triangle with vertices (**A**, **B**, $\mathbf{x}_q$), we obtain [7]

$$(x_q - (x_{tm} + z_{off}\tan\theta_{mq}))^2 + z_q^2 = l_{mq,wall}^2 + l_{mq,air,2}^2 - 2l_{mq,wall}l_{mq,air,2}\cos(\pi + \psi_{mq} - \theta_{mq}) \tag{8}$$

where ψ_{mq} is given by (6). Eq. (8) is a transcendental equation in the unknown θ_{mq} and can be solved numerically.

PRACTICAL EXAMPLE

For illustration, we apply the beamforming technique described above to real-data collected using a wideband through-the-wall synthetic aperture radar in the Radar Imaging Lab at Villanova

University. An Agilent network analyzer, ENA 5071B, was used to synthesize a 1GHz signal, centered at 2.5 GHz, using 201 frequencies with a step size of 5 MHz. A horn antenna, with an operational bandwidth from 1 to 12.4 GHz, was used as the transceiver and mounted on a Field Probe Scanner to synthesize an 85-element line array with an inter-element spacing of 2.23cm. Hanning weighting was applied to the array elements. A 3.65m x 2.54m segment of a 7.6cm thick plywood wall with a dielectric constant of 2.22 was placed 0.7m in front of the antenna baseline. A metal pipe of 0.5m length and 0.1m diameter, located at (9.14cm, 4.24m) in the (x, z)-plane, was used as the target. The corresponding beamformed image is provided in Fig. 3, which clearly shows not only the wall and the target, but also returns resulting from multiple reflections within the wall. We observe from Fig. 3 that the mainlobe of the target response is centered at (9.14cm, 4.24m) and thus the target has been accurately located behind the wall.

EXTENSIONS

The work described earlier for two-dimensional (2-D) through-the-wall imaging using line arrays can be extended to three-dimensional (3-D) imaging using planar arrays, which provides, in addition to range, valuable information about the target extent in length, height, and width. This additional feature is instrumental to effective target identification/classification. For 3-D imaging, the region of interest is divided into volume pixels (voxels) in x, y, and z dimensions. If both the image voxel and the transceiver are at the same height, then the focusing delay computation reduces to an equivalent 2-D problem. If, on the other hand, the image voxel and the transceiver assume different heights, a rotation transform can be applied so that in the new coordinate system, the m-th transceiver and the q-th voxel assume the same height. This transformation preserves the angle of incidence, and as such, does not alter the traveling distances outside and inside the wall. In both cases, (5)-(7) can then be used to compute the traveling distances and hence the corresponding focusing delays for 3-D imaging. Detailed analysis of 3-D imaging through a single uniform wall is presented in [8].

The algorithm discussed earlier assumes knowledge of the wall thickness and dielectric constant. However, in typical through-the-wall imaging scenarios, the wall characteristics may not be known exactly. Ambiguities in wall parameters tend to smear and blur the image and cause the imaged targets to shift away from their true positions. If unaccounted for, the image degradations reduce the accuracy and reliability of TWRI and compromise the integrity of the system. Various techniques for mitigating the detrimental effects of unknown walls on imaging quality and

reliability have been proposed [9]-[10]. One such technique is based on wideband beamforming, and uses the bias in imaged target location, when incorporating incorrect walls. It requires the use of two or more different array structures, and corrects for wall ambiguities by utilizing the distinctions in the respective location bias trajectories [9]. Another technique uses the effect of wall ambiguities on the target spread and intensity profile to focus the image and correct for shifts in locations of imaged stationary targets [10].

CONCLUSIONS: WHAT WE HAVE LEARNED

We have presented a wideband synthetic aperture beamformer for imaging through a single uniform wall with known characteristics. The design of the beamformer incorporates the effects of the wall through which the imaging system is looking. These effects include the reduction in propagation speed, and more importantly, wave refraction. We provided an example based on real-data collected in a semi-controlled environment, which shows the effectiveness of the through-the-wall technique. We also briefly discussed an approach for extending the two-dimensional design to three-dimensional through-the-wall beamforming and commented on two techniques for imaging in the presence of walls with unknown characteristics.

AUTHORS

Moeness G. Amin (moeness.amin@villanova.edu) is a Professor in the Department of Electrical and Computer Engineering and the Director of the Center for Advanced Communications at Villanova University, Villanova, PA. His research interests are in the areas of wireless communications, time-frequency analysis, smart antennas, interference cancellation in broadband communication platforms, direction finding, radar imaging, and channel equalization. He is a Fellow of the IEEE and the SPIE societies.

Fauzia Ahmad (fauzia.ahmad@villanova.edu) is a Research Associate Professor and the Director of the Radar Imaging Lab at Villanova University, Villanova, PA. Her research interests are in the areas of radar imaging, array signal processing, and source localization. She is a Senior member of IEEE.

REFERENCES

1. M. Farwell et al., “US Army Sense Through the Wall System Development and Design Considerations,” *Journal of the Franklin Institute,* March 2008.

2. S. E. Borek, “An overview of through the wall surveillance for homeland security,” in *Proc. 34th Applied Imagery and Pattern Recognition Workshop*, Oct. 2005.
3. E. Ertin and R. Moses, “Through-the-wall SAR attributed scattering center feature estimations,” *Proceedings of the 2008 IEEE International Conference on Acoustics, Speech, and Signal Processing*, April 2008.
4. A. Lin and H. Ling, “Through-wall measurements of a Doppler and direction-of-arrival (DDOA) radar for tracking indoor movers,” *Proceedings of the 2005 IEEE AP-S International Symposium*, vol. 3B, July 2005, pp. 322-325.
5. R. M. Narayanan, “Through Wall Radar Imaging Using UWB Noise Waveforms,” *Journal of the Franklin Institute*, March 2008.
6. P. Withington, H. Fluhler, S. Nag, “Enhancing homeland security with advanced UWB sensors,” *IEEE Microwave magazine*, vol. 4, no. 3, 2003, pp. 51-58.
7. F. Ahmad and M. Amin, “Noncoherent approach to through-the-wall radar localization,” *IEEE Trans. Aerosp. Electron. Syst*., vol. 42, no. 4, Oct. 2006, pp. 1405–1419.
8. F. Ahmad, Y. Zhang, and M. Amin, “Three-Dimensional Wideband Beamforming for Imaging through a Single Wall,” to appear in *GeoSci. Remote Sens. Letters*., 2008.
9. G. Wang and M. G. Amin, “Imaging through unknown walls using different standoff distances,” *IEEE Trans. Signal Process.*, vol. 54, no. 10, Oct. 2006, pp. 4015-4025.
10. F. Ahmad, M. G. Amin, and G. Mandapati, “Autofocusing of through-the-wall radar imagery under unknown wall characteristics,” *IEEE Trans. Image Process.*, vol. 16, no. 7, July 2007.

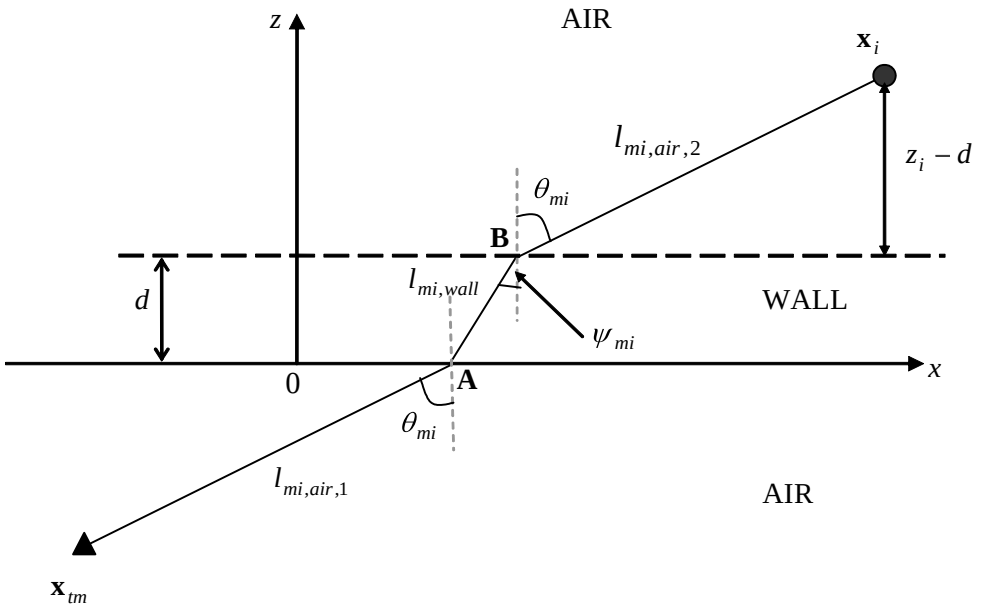

Fig. 1. Geometry for computation of traveling distances from the *m*-th transceiver to $\mathbf{x}_i$, where *i*=*p* for target location and *i*=*q* for *q*-th pixel location.

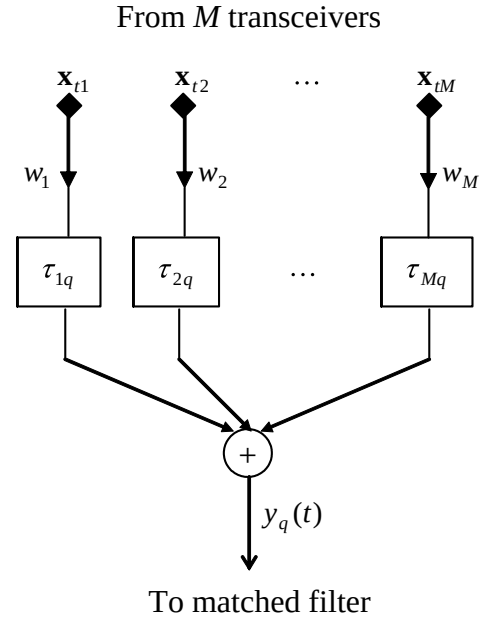

Fig. 2. Block Diagram of the Beamformer

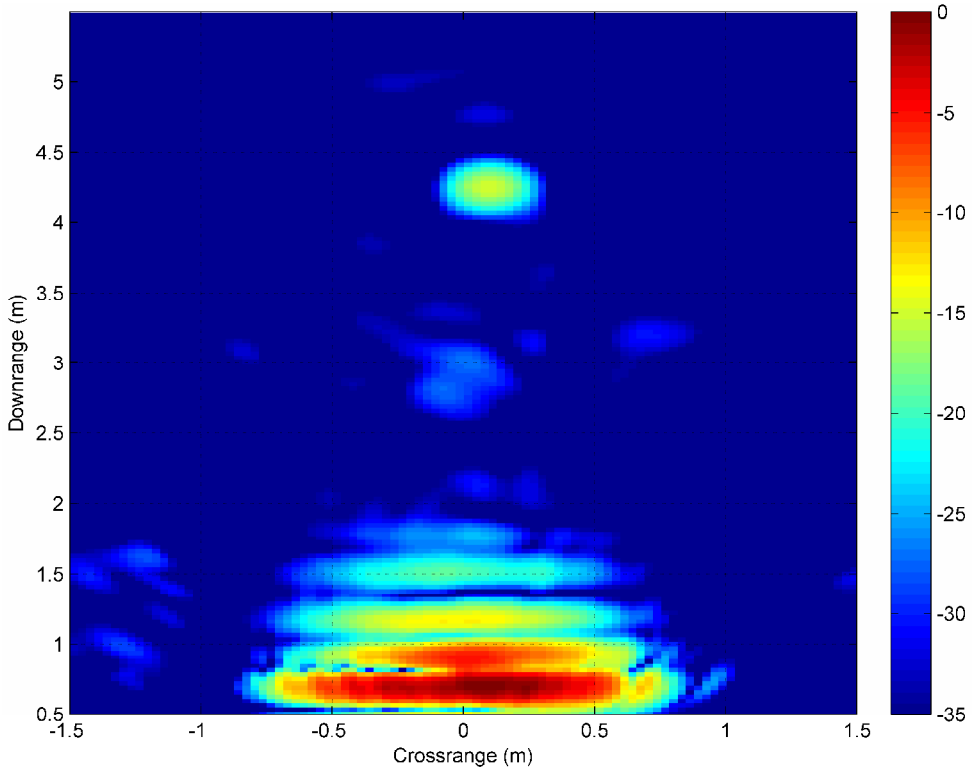

Fig. 3: Image of metal pipe behind a plywood wall.